



An inverse method to determine the elastic properties of the interphase between the aggregate and the cement paste

Z. Hashin^a, P.J.M. Monteiro^{b,*}

^a*Faculty of Engineering, Tel Aviv University, Tel Aviv, Israel*

^b*Department of Civil and Environmental Engineering, University of California, Berkeley, 725 Davis Hall, Berkeley, CA 94720, USA*

Received 23 August 1999; accepted 1 March 2002

Abstract

Concrete is a three-phase material consisting of cement paste matrix, discrete inclusions of rock (aggregate), and an interfacial transition zone (ITZ) between the matrix and the inclusions. We model the material as a composite formed by a matrix with embedded spherical particles; each surrounded by a concentric spherical shell. Effective elastic moduli of this composite are evaluated on the basis of the generalized self-consistent scheme (GSCS). This formulation is used to solve the inverse problem of determining the elastic moduli of the ITZ from experimentally known elastic properties of the composite. © 2002 Published by Elsevier Science Ltd.

Keywords: Elastic moduli; Interfacial transition zone; Micromechanics; Modeling; Mortar

1. Introduction

Concrete is a complex material which consists of aggregate particles dispersed in a porous cement paste. Farran [1] observed that the packing of cement grains close to an aggregate surface was lower than their packing within the cement paste matrix. After studying the contact between cement paste matrix and aggregates with various mineralogies, Farran [2] proposed the existence of a “transition aureole” around the aggregate particles. This “interfacial transition zone” (ITZ) is characterized by a higher porosity than that of the cement paste and is created by a wall-effect initiated by the aggregate surface. Internal bleeding of fresh concrete can also contribute to a localized higher water-to-cement ratio, which permits the precipitation of larger crystals and, in the case of calcium hydroxide, with a preferred orientation. Originally, the interface between aggregate and cement paste was studied by use of “composite specimens” prepared by casting cement paste on top of a polished substrate. Using SEM analysis, Hadley [3] described the transition zone as consisting of a duplex film, formed by calcium hydroxide crystals and C-S-H, attached

to the aggregate surface, and a porous cement paste with larger porosity than that of the bulk cement paste. Grandet and Ollivier [4] used an ingenious X-ray diffraction technique to determine the thickness of the transition zone which they defined as the distance from the aggregate interface where the calcium hydroxide crystals no longer displayed preferred orientation. The major criticism of these pioneering works was the use of the idealized “composite specimens” described above to simulate the transition zone. Naturally, in this simplified configuration, the effects of mixing and the interactions between aggregate particles were not included. Many of these limitations were overcome by Scrivener and Pratt [5,6] who studied the microstructure of the transition zone in real concrete specimens using backscattered electron microscopy associated with computerized image processing. Their work confirmed the existence of a porosity gradient between the aggregate and the bulk cement paste.

Many experiments have been performed to study the effect of mineral admixtures, time and type of cement on the microstructure of the ITZ, leading to a more fundamental understanding of concrete behavior and providing a scientific basis for the development of high-performance concrete. However, the quantification of the effect of the transition zone on the mechanical properties has proved to be difficult. The thickness of the transition zone is small, ranging from 15 to 40 μm , and it is difficult to isolate its effect on the

* Corresponding author. Tel.: +1-510-643-8251; fax: +1-510-643-5264.

E-mail address: paulmont@euler.berkeley.edu (P.J.M. Monteiro).

properties of concrete which are also affected by aggregate size, texture and gradation and by the complex nature of the cement paste which is time and temperature dependent. Traditional modeling to obtain elastic properties described concrete as a two-phase composite material consisting of spherical aggregate inclusions embedded in a cement paste matrix. The limitations of a two-phase model have been pointed out by Nielsen and Monteiro [7] who showed that many of the experimental results obtained by Hirsch [8] violated the Hashin–Strikman (HS) [9] bounds, which are valid for two-phase statistically isotropic materials of any phase geometry. They proposed that concrete be modeled as a three-phase material consisting of aggregate particles, surrounded by a transition zone, embedded in the cement

paste matrix. Lutz [10] applied a model in which the elastic moduli in the transition zone vary according to a radial power function. This model was developed by Lutz and Monteiro [11] and by Lutz et al. [12] to estimate the radial bulk modulus variation within the transition zone. Ramesh et al. [13] employed a four-phase composite model consisting of aggregate, transition zone, matrix and equivalent homogeneous medium. This model has become known as the generalized self-consistent scheme (GSCS) and has been used in the form developed in Ref. [13] by Christensen and Lo [14]. In the present work, we also employ the GSCS but in inverse fashion. Our purpose is to determine the interphase elastic properties on the basis of experimentally known effective elastic properties of the composite.

2. Analysis

2.1. General

The material will be modeled as a composite consisting of a matrix in which are embedded spherical particles, each of which is surrounded by a concentric spherical shell which will be called the *interphase*. Matrix, particle and interphase materials are considered elastic isotropic and the entire composite is assumed to be statistically homogeneous and isotropic. We shall first consider the classical problem of analytical determination of the effective elastic properties of the composite in terms of constituent properties and internal geometry. On that basis we shall then be concerned with determination of interphase properties in terms of particle and matrix properties and effective properties.

There is a very large literature on effective elastic properties of spherical particle composites without an interphase. For review, see, e.g., Ref. [15]. We believe that the appropriate method for treatment of the present problem is the GSCS. The method has first been correctly applied to the case when there is no interphase in Ref. [16] and has been simplified and clarified in Ref. [14]. It has been extended to the case of particles surrounded by any number of interphase layers in Ref. [17] and to the case of imperfect interface between particles and matrix in Ref. [18]. We shall proceed here according to the point of view adopted in Ref. [18], which we consider to be physically more convincing than the various assumptions underlying Refs. [14,16] though, mathematically, all are equivalent.

The effective elastic moduli tensor \mathbf{C}^* of a composite is defined by the relation (Eq. (1))

$$\sigma = \mathbf{C}^* \bar{\epsilon} \quad (1)$$

where the overbar denotes average over representative volume element and σ and ϵ are stress and strain, respectively. The homogeneous boundary conditions

$$\mathbf{u}(S) = \bar{\epsilon} \mathbf{x} \quad (2a)$$

or

$$\mathbf{T}(S) = \bar{\sigma} \mathbf{n} \quad (2b)$$

induce in a statistically homogeneous composite the average strain $\bar{\epsilon}$ or average stress $\bar{\sigma}$, respectively. Eq. (2a) gives the homogeneous displacement boundary condition while Eq. (2b) gives the homogeneous traction boundary condition over the bounding surface S .

The present composite consists of three phases. Global average stress and strain may be written as weighted averages in the form (Eqs. (3a) and (3b))

$$\bar{\epsilon} = \bar{\epsilon}^{(1)} v_1 + \bar{\epsilon}^{(2)} v_2 + \bar{\epsilon}^{(3)} v_3 \quad (3a)$$

$$\bar{\sigma} = \bar{\sigma}^{(1)} v_1 + \bar{\sigma}^{(2)} v_2 + \bar{\sigma}^{(3)} v_3 = (\mathbf{C}^{(1)} \bar{\epsilon}^{(1)} v_1 + \mathbf{C}^{(2)} \bar{\epsilon}^{(2)} v_2 + \mathbf{C}^{(3)} \bar{\epsilon}^{(3)} v_3) \quad (3b)$$

where v is volume fraction, \mathbf{C} with superscript denotes elastic phase moduli tensor and an average with superscript denotes a phase average. Eliminating $\epsilon^{(1)}$ from (1,3) we have

$$\mathbf{C}^* \bar{\epsilon} = \mathbf{C}^{(1)} \bar{\epsilon} + (\mathbf{C}^{(2)} - \mathbf{C}^{(1)}) \bar{\epsilon}^{(2)} v_2 + (\mathbf{C}^{(3)} - \mathbf{C}^{(1)}) \bar{\epsilon}^{(3)} v_3. \quad (4)$$

We consider the case when the phases are all isotropic and the composite is statistically isotropic. Then each of the moduli tensors is isotropic and is completely characterized by a bulk modulus K and shear modulus G . Then Eq. (4) assumes the form

$$\begin{aligned} K^* &= K_1 + (K_2 - K_1)(\bar{\epsilon}^{(2)}/\bar{\epsilon})v_2 + (K_3 - K_1)(\bar{\epsilon}^{(3)}/\bar{\epsilon})v_3 \\ G^* &= G_1 + (G_2 - G_1)(\bar{e}_{ij}^{(2)}/e_{ij})v_2 + (G_3 - G_1)(\bar{e}_{ij}^{(3)}/\bar{e}_{ij})v_3 \end{aligned} \quad (5)$$

(no sum on ij) where ϵ and e_{ij} are isotropic and deviatoric components of a tensor ϵ_{ij} , thus (Eq. (6))

$$\epsilon_{ij} = \epsilon \delta_{ij} + e_{ij}. \quad (6)$$

In the following, Phases 1, 2, 3 will be identified as Matrix 1, Particles 2 and Interphase i , respectively. We use the GSCS in order to determine the phase averages in Eq. (5), approximately. To do this, consider a composite sphere which consists of inner spherical particle core and concentric spherical interphase and matrix shells. The relative volume fractions of phase materials in this sphere are chosen as the phase volume fractions of the composite. The fundamental premise of the GSCS is that for purpose of phase average evaluation it may be assumed that the composite sphere is embedded in the effective material which has properties K^* and G^* , to be determined. The composite is subjected to average strain $\bar{\epsilon}_{ij}$. This defines a four-phase boundary value problem (Fig. 1) in which the displacements at infinity have the form

$$u_i(\mathbf{x})_{x \rightarrow \infty} = \bar{\epsilon}_{ij} x_j. \quad (7)$$

The strain phase averages in Eq. (5) are to be evaluated from this boundary value problem. Note, however, that originally [3], the GSCS was formulated in terms of a postulated energy equality. It is believed that the present approach is physically more convincing and it has been shown [18], that it is mathematically equivalent. Furthermore, the computational effort to derive the results is considerably smaller than with the energy approach. Additional simplicity has been achieved by formulation of the shear problem in terms of axisymmetric elasticity, as has also been done in Ref. [16].

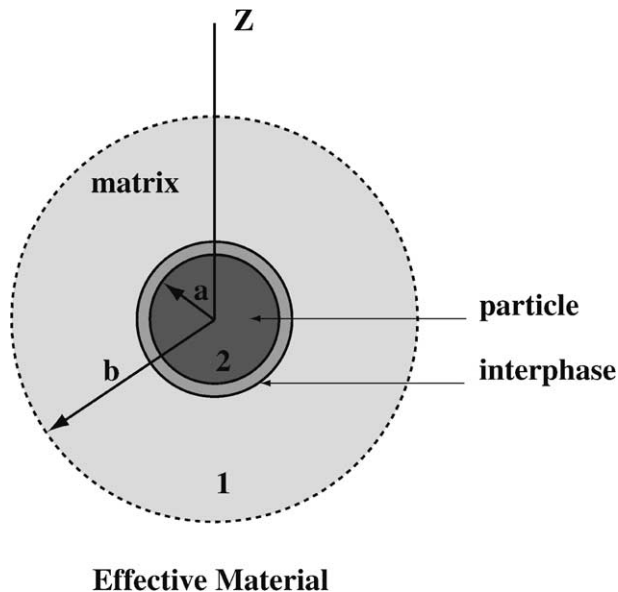


Fig. 1. Boundary value problem for GSCS.

2.2. Effective bulk modulus

In order to compute for the effective bulk modulus, the average strain in Eq. (7) is taken as isotropic, thus

$$u_i(\mathbf{x})_{x \rightarrow \infty} = \bar{\epsilon} x_i. \quad (8)$$

This implies that the remote displacement is in the radial direction and therefore the four-phase boundary value problem (Fig. 1) is radially symmetric. Thus, $u_r = u_r(r)$, $u_\phi = u_\theta = 0$, and Eq. (8) assumes the form (Eq. (9))

$$u_r(r \rightarrow \infty) = \bar{\epsilon} r. \quad (9)$$

Because of the radial symmetry, the general GSCS procedure outlined above becomes an elementary matter. However, it is even easier to proceed in a different way. The GSCS for a two-phase particle composite, i.e., when there is no interphase, yields the effective bulk modulus result [14,15]

$$K^* = K_1 + \frac{v_2}{1/(K_2 - K_1) + 3v_1/(3K_1 + 4G_1)} \quad (10)$$

where v_1 , v_2 are the volume fractions. Now, it is well known that a composite two-phase sphere is elastically equivalent to a homogeneous sphere with bulk modulus given by Eq. (10), where 2, 1 are inner core and surrounding shell materials, respectively. Thus, in the four-phase boundary value problem, the inner composite sphere can be (rigorously) replaced by such an equivalent homogeneous sphere without changing the elastic fields in the matrix and effective material regions. Therefore, the equivalent bulk modulus of the inner composite sphere is given by (Eq. (11))

$$K_e = K_i + \frac{v_2/(v_1 + v_2)}{1/(K_2 - K_i) + [3v_i/(v_i + v_2)]/(3K_1 + 4G_1)} \quad (11)$$

It then follows from Eq. (10) that the effective bulk modulus is given by

$$K^* = K_1 + \frac{v_1 + v_2}{1/(K_e - K_1) + 3v_1/(3K_1 + 4G_1)} \quad (12)$$

2.3. Effective shear modulus

In order to compute the effective shear modulus, the average strain in Eq. (7) is taken as deviatoric, thus

$$u_i(\mathbf{x})_{(x \rightarrow \infty)} = \bar{\epsilon}_{ij} x_j. \quad (13)$$

It has been customary to apply Eq. (13) in the form of pure shear. In spherical coordinates, this leads to a boundary value problem devoid of symmetry where all fields depend on r , φ and θ . Much simplification is achieved if the deviatoric strain (Eq. (14))

$$[\bar{\epsilon}] = \begin{bmatrix} -\beta & 0 & 0 \\ 0 & -\beta & 0 \\ 0 & 0 & 2\beta \end{bmatrix} \quad (14)$$

and therefore Eq. (13) assumes the form

$$u_1 = -\beta x_1 \quad u_2 = -\beta x_2 \quad u_3 = 2\beta x_3 \quad (15)$$

Converting Eq. (15) to spherical coordinates, we have (Eq. (16))

$$u_r = 2\beta r P(\cos\theta) \quad u_\theta = \beta r \dot{P}(\cos\theta) \quad u_\varphi = 0 \quad (16)$$

where P is the second Legendre polynomial. Thus (Eq. (17))

$$P(\cos\theta) = P_2(\cos\theta) = \frac{1}{2}(3\cos^2\theta - 1) \quad \dot{P}(\cos\theta) = dP_2/d\theta = -3\cos\theta\sin\theta. \quad (17)$$

Therefore, the boundary problem is axisymmetric relative to the x_3 axis. The solution to such problems is well known (see e.g., Ref. [19]), and is given for the present case as (Eq. (18))

$$\begin{aligned} u_r &= \beta \left[12\nu\rho^2 A + 2B + \frac{2(5-4\nu)}{\rho^3} C - \frac{3}{\rho^5} D \right] rP \\ u_\theta &= \beta \left[(7-4\nu)\rho^2 A + B + \frac{2(1-2\nu)}{\rho^3} C + \frac{D}{\rho^5} \right] r\dot{P} \\ \sigma_{rr} &= 2\beta G \left[-6\nu\rho^2 A + 2B - \frac{4(5-\nu)}{\rho^3} C + \frac{12}{\rho^5} D \right] rP \\ \sigma_{r\theta} &= 2\beta G \left[(7+2\nu)\rho^2 A + B + \frac{2(1+\nu)}{\rho^3} C - \frac{4}{\rho^5} D \right] r\dot{P} \end{aligned} \quad (18)$$

where $\rho = r/a_2$, ν is the Poisson's ratio and A , B , C , D are unknown constants. There are four such solutions for the four different regions of the boundary value problem which will be labeled 0 for the external effective region and 1, i , 2 for the matrix, interphase and particle regions, respectively. The four solutions must satisfy the following boundary and interface conditions

$$\begin{aligned} u_r^0 &= 2\beta rP & u_\theta^0 &= \beta r\dot{P}_{r \rightarrow \infty} \\ u_r^0(a_1, \theta) &= u_r^1(a_1, \theta) & u_\theta^0(a_1, \theta) &= u_\theta^1(a_1, \theta) \\ \sigma_{rr}^0(a_1, \theta) &= \sigma_{rr}^1(a_1, \theta) & \sigma_{r\theta}^0(a_1, \theta) &= \sigma_{r\theta}^1(a_1, \theta) \\ u_r^1(a_i, \theta) &= u_r^i(a_i, \theta) & u_\theta^1(a_i, \theta) &= u_\theta^i(a_i, \theta) \\ \sigma_{rr}^1(a_i, \theta) &= \sigma_{rr}^i(a_i, \theta) & \sigma_{r\theta}^1(a_i, \theta) &= \sigma_{r\theta}^i(a_i, \theta) \\ u_r^i(a_2, \theta) &= u_r^2(a_2, \theta) & u_\theta^i(a_2, \theta) &= u_\theta^2(a_2, \theta) \\ \sigma_{rr}^i(a_2, \theta) &= \sigma_{rr}^2(a_2, \theta) & \sigma_{r\theta}^i(a_2, \theta) &= \sigma_{r\theta}^2(a_2, \theta) \\ u_r^2(0, \theta) &= u_\theta^2(0, \theta) = 0. \end{aligned} \quad (19)$$

Since each of the solutions for the different regions contains four unknown constants, there are in all 16 unknowns which are uniquely determined by the 16 equations (Eq. (19)). In order to satisfy the first two and the last two equations, we must have

$$\begin{aligned} A_0 &= 0 & B_0 &= 1 \\ C_p &= 0 & D_p &= 0. \end{aligned} \quad (20)$$

This leaves 12 equations for the remaining 12 constants. These equations can be expressed in the general form

$$\begin{aligned}
 a_{kl}A_l &= b_k \quad k, l = 1, 2 \dots 12 \\
 C_0, D_0 &= A_1, A_2 \quad A_m, B_m, C_m, D_m = A_3, A_4, A_5, A_6 \\
 A_i, B_i, C_i, D_i &= A_7, A_8, A_9, A_{10} \quad A_p, B_p = A_{11}, A_{12}.
 \end{aligned} \tag{21}$$

The detailed values of a_{kl} and b_k are given in Appendix A. Note that some of these coefficients depend on G^* and ν^* or equivalently on G^* and K^* . Since these are not known, there are altogether 14 unknowns and there are precisely 14 equations, the second of Eqs. (5), (12) and (21). Manipulation of the equations as done in Ref. [18] leads to the result

$$C_0 = 0. \tag{22}$$

Expressing C_0 from Eqs. (19)–(22) leads to the determinantal equation

$$D = \begin{vmatrix}
 b_1 & a_{12} & a_{13} & a_{14} & a_{15} & a_{16} & 0 & 0 & 0 & 0 & 0 & 0 \\
 b_2 & a_{22} & a_{23} & a_{24} & a_{25} & a_{26} & 0 & 0 & 0 & 0 & 0 & 0 \\
 \mathbf{b}_3 & \mathbf{a}_{32} & a_{33} & a_{34} & a_{35} & a_{36} & 0 & 0 & 0 & 0 & 0 & 0 \\
 \mathbf{b}_4 & \mathbf{a}_{42} & a_{43} & a_{44} & a_{45} & a_{46} & 0 & 0 & 0 & 0 & 0 & 0 \\
 0 & 0 & a_{53} & a_{54} & a_{55} & a_{56} & \mathbf{a}_{57} & \mathbf{a}_{58} & \mathbf{a}_{59} & \mathbf{a}_{510} & 0 & 0 \\
 0 & 0 & a_{63} & a_{64} & a_{65} & a_{66} & \mathbf{a}_{67} & \mathbf{a}_{68} & \mathbf{a}_{69} & \mathbf{a}_{610} & 0 & 0 \\
 0 & 0 & a_{73} & a_{74} & a_{75} & a_{76} & \mathbf{a}_{77} & \mathbf{a}_{78} & \mathbf{a}_{79} & \mathbf{a}_{710} & 0 & 0 \\
 0 & 0 & a_{83} & a_{84} & a_{85} & a_{86} & \mathbf{a}_{87} & \mathbf{a}_{88} & \mathbf{a}_{89} & \mathbf{a}_{810} & 0 & 0 \\
 0 & 0 & 0 & 0 & 0 & 0 & \mathbf{a}_{97} & \mathbf{a}_{98} & \mathbf{a}_{99} & \mathbf{a}_{910} & a_{911} & a_{912} \\
 0 & 0 & 0 & 0 & 0 & 0 & \mathbf{a}_{107} & \mathbf{a}_{108} & \mathbf{a}_{109} & \mathbf{a}_{1010} & a_{1011} & a_{1012} \\
 0 & 0 & 0 & 0 & 0 & 0 & \mathbf{a}_{117} & \mathbf{a}_{118} & \mathbf{a}_{119} & \mathbf{a}_{1110} & a_{1111} & a_{1112} \\
 0 & 0 & 0 & 0 & 0 & 0 & \mathbf{a}_{127} & \mathbf{a}_{128} & \mathbf{a}_{129} & \mathbf{a}_{1210} & a_{1211} & a_{1212}
 \end{vmatrix} = 0. \tag{23}$$

The values of the elements of this determinant are given in Appendix A. The bold-faced elements in the first and second columns of the determinant are the only ones which involve the effective property $g^* = G^*/G_1$ and other effective properties do not appear in the determinant. Therefore, if the unknown is g^* , development of the determinant leads to the quadratic equation (Eq. (24))

$$D(g^*) = Ag^{*2} + 2Bg^* + C = 0 \tag{24}$$

where the coefficients A , B and C may be obtained by numerical development of the determinant or in terms of the values of D for $g^* = \{-1, 0, 1\}$. Then (Eq. (25))

$$\begin{aligned}
 A &= \frac{1}{2}[D(1) + D(-1)] - D(0) \\
 B &= \frac{1}{4}[D(1) - D(-1)] \\
 C &= D(0).
 \end{aligned} \tag{25}$$

The fundamental Eq. (22) has been derived in Ref. [3] on the basis of the assumption that the elastic energy stored in the embedded composite sphere is given by the macro-energy density of the composite multiplied by the sphere volume. It has been shown in Ref. [4] that this equation is also obtained when assuming that the average strain in the composite sphere is the same as the average strain in the composite. Both assumptions are somewhat arbitrary for the embedded composite sphere is *not* a representative volume element of the composite. The point of view adopted here is that the embedded composite sphere boundary value problem is a device to calculate, approximately, phase strain averages as needed for Eq. (5). All of these different approaches result in Eq. (22) and are thus mathematically equivalent.

If the interphase properties G_i and ν_i are the unknowns, while the effective and other phase properties are known, then both Eqs. (12) and (23) are needed. Note that only the elements in the 7th to 10th columns of Eq. (23), emphasized in bold face, involve the interphase properties. If all other quantities are numerically known, we obtain the two simultaneous equations

$$\begin{aligned} c_{00} + c_{10}g_{i1} + c_{20}g_{i1}^2 + c_{30}g_{i1}^3 + c_{40}g_{i1}^4 + c_{11}g_{i1}\nu_i + c_{21}g_{i1}^2\nu_i + c_{31}g_{i1}^3\nu_i + c_{41}g_{i1}^4\nu_i + c_{12}g_{i1}\nu_i^2 + c_{22}g_{i1}\nu_i^2 + c_{32}g_{i1}^3\nu_i^2 \\ + c_{42}g_{i1}^4\nu_i^2 = 0 \\ b_{00} + b_{01}\nu_i + b_{02}\nu_i^2 + b_{10}g_{i1} + b_{11}g_{i1}\nu_i + b_{12}g_{i1}\nu_i^2 + b_{20}g_{i1}^2 + b_{21}g_{i1}^2\nu_i + b_{22}g_{i1}^2\nu_i^2 = 0 \end{aligned} \quad (26)$$

where $g_{i1} = G_i/G_1$.

The first equation follows from the development of the determinant in Eq. (23) and the second equation follows from Eq. (12). The coefficients in these equations are numerically known and the equations can only be solved numerically.

3. Evaluation of interphase properties

There exists a significant amount of information about the dependence of Young's modulus of concrete on the amount of aggregate concentration. Unfortunately, there is only a very limited amount of experimental results where two effective elastic moduli are determined as a function of aggregate concentration. We shall use the experimental data obtained by Wang et al. [20] who measured the elastic moduli of saturated mortar specimens, which contained various amounts of sand inclusions. The elastic properties of the constituents are given in Table 1. Table 2 gives the results of the effective properties (in GPa) measured for various volume fractions ν_2 of sand particles in a Portland cement mortar. The average diameter of the sand particles was approximately 850 μm . Table 3 below shows the values of the interphase properties extracted on the basis of Eqs. (23) and (26) and the information (Eqs. (27) and Table 1) for the various interphase thickness.

We shall use experimental data for saturated cement mortar generated in Ref. [20].

Table 2 gives the results of effective properties (also in GPa), measured for various volume fractions ν_2 of sand particles. The average diameter of the sand particles was 850 μm ($1 \mu\text{m} = 10^{-6} \text{ m}$) while the interphase thickness was estimated as 25 μm .

Previous conducted microscopy studies of the ITZ indicate that the zone has porosity gradients, the presence of calcium hydroxide with texture near the aggregate and a higher concentration of ettringite near the interface. These heterogeneities originate a gradient of properties within the interphase. The present model maps this complex gradient into a domain where the interphase has uniform properties, whereby the width of this equivalent interphase becomes distinct from the physical thickness of the ITZ measured by image analysis. Therefore, we study the interphase moduli as a function of the assumed width of the interphase. Table 3 shows the values of the interphase properties derived from Eqs. (23) and (26), and various interphase thicknesses.

The Young's modulus of the interphase, E_{i1} , can be computed from the values of shear modulus and Poisson's ratio by using the following equation:

$$E_{i1} = 2g_{i1}(1 + \nu_i). \quad (27)$$

The shear and Young's moduli of the interphase are about 50% of those of the original bulk cement paste, while the

Table 1
Elastic properties of the constituents (in GPa)

Constituent	K	G
Cement paste (1)	22.51	11.8
Sand particles (2)	44.0	37.0

Table 2
Experimental values of the elastic moduli of mortar measured for various volume fractions of sand

ν_2	K^*	G^*
0.15	24.14	13.35
0.27	26.81	14.87
0.40	27.69	16.91
0.52	29.96	19.26
0.65	30.12	20.23

Table 3
Shear modulus, g_{i1} , and Poisson's ratio, ν_i , of the interface obtained from Eqs. (23)–(26)

v_2	$t_i = 24 \mu\text{m}$		$t_i = 26 \mu\text{m}$		$t_i = 28 \mu\text{m}$	
	g_{i1}	ν_i	g_{i1}	ν_i	g_{i1}	ν_i
0.15	0.467	0.316	0.489	0.314	0.509	0.313
0.27	0.475	0.400	0.498	0.394	0.520	0.389
0.40	0.553	0.313	0.574	0.311	0.594	0.309
0.52	0.612	0.311	0.632	0.309	0.650	0.307

bulk modulus is on the order of 70% of the original bulk cement paste. Using microstructural simulations of the mortar, Neubauer et al [21] estimated that the Young's modulus of the ITZ is of the same order of magnitude of the present analysis. As shown in Table 3 for the range of interphase thickness analyzed, the interphase shear modulus increases as the volume fraction of the particles grows. This increase is easily explained: the interphase results when the wall-effect is generated as a result of the sand particles. Because of this geometric constraint, the cement grains cannot pack efficiently near the aggregate surface, leading to a higher concentration of water in the interphase. Once the total amount of mixing water is constant, less water will be present in the matrix, producing an increase in the matrix stiffness once hydration starts. The present model assumes that the elastic moduli of the matrix are constant as there is little experimental data on this increase. The elastic moduli of the interphase are the open parameters in the present inversion scheme. Consequently, the resulting values of the moduli of the interphase increase to compensate for the fact that the moduli of the matrix are not allowed to increase as the volume fraction of the interphase grows. As expected, the increase is more notable in the case of higher particle volume fractions.

Note that the elastic moduli of the interphase were obtained using a fully deterministic inversion model. A more realistic determination of the interphase properties should include a reliability analysis of the model identification process. The present mathematical model contains two main sources of errors.

3.1. Simplification errors

A mathematical model seldom captures all the complexities existing in the physical world. Recognizing this fundamental limitation, the most significant parameters are selected and the predictions checked against available experimental evidence.

3.2. Experimental measurement errors

The quality of the inversion process is dependent on the precision of the experimental data. In the present model, the experimental errors are associated with determining the

volume fraction of the phases and the elastic moduli of the mortar, cement paste and aggregate.

The inversion scheme is also sensitive to the degree of heterogeneity of the system. In the present analysis, the stiffness ratio of particles to matrix is about 2 for bulk modulus and about 3 for shear modulus. Calculations show that the interphase shear modulus is about half that of matrix shear modulus. Since interphase volume fraction is small, the actual value of its shear modulus will not significantly affect the effective shear modulus unless the interphase stiffness is extreme, i.e., very small or very large. This is not the case for mortar. The effective shear modulus is a weak function of interphase shear modulus. Therefore, a small change or error in determining the effective modulus may lead to a large error in calculating the interphase modulus. This only reinforces the need to obtain precise measurements of elastic moduli of mortar and concrete as a function of aggregate volume fractions.

As precise experimental results become available, the present formulation can provide quantitative information on the changes of ITZ moduli when special admixtures are used in concrete. For instance, it is well known that silica fume increases the mechanical properties of concrete and it has been proposed that this mineral admixture produces a significant improvement on the properties of the ITZ. The present methodology permits to quantify the changes in the ITZ in silica fume concrete. Similarly, it will be possible to measure the changes in the ITZ when dry lightweight aggregate is used in the production of concrete.

4. Conclusions

We developed a model for concrete where the aggregate particle is surrounded by ITZ. The elastic moduli of the aggregate, cement paste matrix and transition zone are assumed to be constant. The elastic moduli of the cement paste and aggregate are often known but no experimental data exist on the elastic moduli of the transition zone. We reported an efficient methodology of estimating these values from experimental data on Portland cement mortar samples cast with varying amounts of sand concentrations. The model presented herein predicts that the shear and Young's moduli of ITZ is $\sim 50\%$ of those of the bulk cement paste, where calculations are based upon experimental data collected by Wang et al. [20].

Acknowledgments

The authors are grateful for the financial support given by Lafarge. They also wish to acknowledge Drs. A. Capmas and K. Scrivener for helpful discussion.

Appendix A.

The values of the determinant elements are given below

$a_{11} = -2(5 - 4\nu^*)/\rho_1^3$	$a_{12} = 3/\rho_1^5$	$a_{13} = 12\nu_1\rho_1^2$	$a_{14} = 2$
$a_{21} = -2(1 - 2\nu^*)/\rho_1^3$	$a_{22} = -1/\rho_1^5$	$a_{23} = (7 - 4\nu_1)\rho_1^2$	$a_{24} = 1$
$a_{31} = 4(5 - \nu^*)g^*/\rho_1^3$	$a_{32} = -12g^*/\rho_1^5$	$a_{33} = -6\nu_1\rho_1^2$	$a_{34} = 2$
$a_{41} = -2(1 + \nu^*)g^*/\rho_1^3$	$a_{42} = 4g^*/\rho_1^5$	$a_{43} = (7 + 2\nu_1)\rho_1^2$	$a_{44} = 1$
$a_{51} = 0$	$a_{52} = 0$	$a_{53} = 12\nu_1\rho_i^2$	$a_{54} = 2$
$a_{61} = 0$	$a_{62} = 0$	$a_{63} = (7 - 4\nu_1)\rho_i^2$	$a_{64} = 1$
$a_{71} = 0$	$a_{72} = 0$	$a_{73} = -6\nu_1\rho_i^2$	$a_{74} = 2$
$a_{81} = 0$	$a_{82} = 0$	$a_{83} = (7 + 2\nu_1)\rho_i^2$	$a_{84} = 1$
$a_{91} = 0$	$a_{92} = 0$	$a_{93} = 0$	$a_{94} = 0$
$a_{101} = 0$	$a_{102} = 0$	$a_{103} = 0$	$a_{104} = 0$
$a_{111} = 0$	$a_{112} = 0$	$a_{113} = 0$	$a_{114} = 0$
$a_{121} = 0$	$a_{122} = 0$	$a_{123} = 0$	$a_{124} = 0$
$a_{15} = 2(5 - 4\nu_1)/\rho_1^3$	$a_{16} = -3/\rho_1^5$	$a_{17} = 0$	$a_{18} = 0$
$a_{25} = 2(1 - 2\nu_1)/\rho_1^3$	$a_{26} = 1/\rho_1^5$	$a_{27} = 0$	$a_{28} = 0$
$a_{35} = -4(5 - \nu_1)/\rho_1^3$	$a_{36} = 12/\rho_1^5$	$a_{37} = 0$	$a_{38} = 0$
$a_{45} = 2(1 + \nu_1)/\rho_1^3$	$a_{46} = -4/\rho_1^5$	$a_{47} = 0$	$a_{48} = 0$
$a_{55} = 2(5 - 4\nu_1)/\rho_1^3$	$a_{56} = -3/\rho_1^5$	$a_{57} = -12\nu_i\rho_i^2$	$a_{58} = -2$
$a_{65} = 2(1 - 2\nu_1)/\rho_1^3$	$a_{66} = 1/\rho_1^5$	$a_{67} = -(7 - 4\nu_i)\rho_i^2$	$a_{68} = -1$
$a_{75} = -4(5 - \nu_1)/\rho_1^3$	$a_{76} = 12/\rho_1^5$	$a_{77} = 6\nu_i\rho_i^2g_{i1}$	$a_{78} = -2g_{i1}$
$a_{85} = 2(1 + \nu_1)/\rho_1^3$	$a_{86} = -4/\rho_1^5$	$a_{87} = -(7 + 2\nu_i)\rho_i^2g_{i1}$	$a_{88} = -g_{i1}$
$a_{95} = 0$	$a_{96} = 0$	$a_{97} = 12\nu_i$	$a_{98} = 2$
$a_{105} = 0$	$a_{106} = 0$	$a_{107} = 7 - 4\nu_i$	$a_{108} = 1$
$a_{115} = 0$	$a_{116} = 0$	$a_{117} = -6\nu_i$	$a_{118} = 2$
$a_{125} = 0$	$a_{126} = 0$	$a_{127} = 7 + 2\nu_i$	$a_{128} = 1$
$a_{19} = 0$	$a_{110} = 0$	$a_{111} = 0$	$a_{112} = 0$
$a_{29} = 0$	$a_{210} = 0$	$a_{211} = 0$	$a_{212} = 0$
$a_{39} = 0$	$a_{310} = 0$	$a_{311} = 0$	$a_{312} = 0$
$a_{49} = 0$	$a_{410} = 0$	$a_{411} = 0$	$a_{412} = 0$
$a_{59} = -2(5 - 4\nu_i)/\rho_i^3$	$a_{510} = 3/\rho_i^5$	$a_{511} = 0$	$a_{512} = 0$
$a_{69} = -2(1 - 2\nu_i)/\rho_i^3$	$a_{610} = -1/\rho_i^5$	$a_{611} = 0$	$a_{612} = 0$
$a_{79} = 4(5 - \nu_i)g_{i1}/\rho_i^3$	$a_{710} = -12g_{i1}/\rho_i^5$	$a_{711} = 0$	$a_{712} = 0$
$a_{89} = -2(1 + \nu_i)g_{i1}/\rho_i^3$	$a_{810} = 4g_{i1}/\rho_i^5$	$a_{811} = 0$	$a_{812} = 0$
$a_{99} = 2(5 - 4\nu_i)$	$a_{910} = -3$	$a_{911} = -12\nu_2$	$a_{912} = -2$
$a_{109} = 2(1 - 2\nu_i)$	$a_{1010} = 1$	$a_{1011} = -(7 - 4\nu_2)$	$a_{1012} = -1$
$a_{119} = -4(5 - 4\nu_i)$	$a_{1110} = 12$	$a_{1111} = 6\nu_2g_{2i}$	$a_{1112} = -2g_{2i}$
$a_{129} = 2(1 + \nu_i)$	$a_{1210} = -4$	$a_{1211} = -(7 + 2\nu_2)g_{2i}$	$a_{1212} = -g_{2i}$
$b_1 = 2$			
$b_2 = 1$			
$b_3 = 2g^*$			
$b_4 = g^*$			
$b_5 = 0$			
$b_6 = 0$			
$b_7 = 0$			
$b_8 = 0$			
$b_9 = 0$			
$b_{10} = 0$			
$b_{11} = 0$			
$b_{12} = 0$			

Here $\rho_1 = a_1/a_2 = 1/\nu_2^{1/3}$; $\rho_i = a_i/a_2 = [(1 - \nu_1)/\nu_2]^{1/3}$; $g^* = G^*/G_1$; $g_{i1} = G_i/G_1$; $g_{2i} = G_2/G_i$.

References

- [1] J. Farran, C.R. Seances Acad. Sci., Paris 237 (1953) 73.
- [2] J. Farran, Contribution mineralogique a l'etude de l'adherence entre les constituants hydrates des ciments et les materiaux enrobes, *Revue des Matériaux de Construction* 491 (1956) 155–157, 492, 191–209.
- [3] D.H. Hadley, The Nature of the Paste–Aggregate Interface, PhD Thesis, Purdue University, 1972.
- [4] J. Grandet, J.P. Ollivier, Nouvelle methode d'etude des interface ciments-granulats, *Proceedings of the 7th International Congress on Chemistry of Cement*, Editions Septima, Paris vols. III, VII, 1980, pp. 85–89.
- [5] K.L. Scrivener, P.L. Pratt, A preliminary study of the microstructure of the cement paste–aggregate bond in mortars, *Proceedings of the 8th International Congress on the Chemistry of Cement*, Rio de Janeiro vol. III, 1986, pp. 466–471.
- [6] K.L. Scrivener, P.L. Pratt, Characterization of interfacial microstructure, in: J.C. Maso (Ed.), *Interfacial Transition Zone in Concrete*, E&FN Spon, London, 1996, pp. 3–17.
- [7] A.U. Nielsen, P.J.M. Monteiro, Concrete: A three phase material, *Cem. Concr. Res.* 23 (1993) 147–151.
- [8] T.J. Hirsch, Modulus of elasticity of concrete affected by elastic moduli of cement paste matrix and aggregate, *J. Am. Concr. Inst., Proc.* 59 (1962) 427–451.
- [9] Z. Hashin, S. Strikman, A variational approach to the theory of the elastic behavior of multiphase materials, *J. Mech. Phys. Solids* 11 (1963) 127.
- [10] M.P. Lutz, Elastic and Thermoelastic Behavior of Materials with Continuously-Varying Elastic Moduli, PhD dissertation, University of California at Berkeley, 1995.
- [11] M.P. Lutz, P.J.M. Monteiro, Effect of the transition zone on the bulk modulus of concrete, *Mater. Res. Soc. Symp. Proc.* 370 (1995) 413–418.
- [12] M.P. Lutz, P.J.M. Monteiro, R.W. Zimmerman, Inhomogeneous interfacial transition zone model for the bulk modulus of mortar, *Cem. Concr. Res.* 27 (7) (1997) 1113–1122.
- [13] G. Ramesh, E.D. Sotelino, W.F. Chen, Effect of transition zone on elastic moduli of concrete materials, *Cem. Concr. Res.* 26 (1996) 611–622.
- [14] R.M. Christensen, K.H. Lo, Solutions for effective shear properties in three phase sphere and cylinder models, *J. Mech. Phys. Solids* 27 (1979).
- [15] Z. Hashin, Analysis of composite materials—a survey, *J. Appl. Mech.* 50 (1983) 481–505.
- [16] J.C. Smith, Correction and extension of Van der Poel's method for calculating the shear modulus of a particulate composite, *J. Res. Natl. Bur. Stand.* 78A (1974) 355–361.
- [17] E. Herve, A. Zaoui, n-layered inclusion-based micromechanical modelling, *Int. J. Eng. Sci.* 31 (1993) 1–10.
- [18] Z. Hashin, Thermoelastic properties of particulate composites with imperfect interface, *J. Mech. Phys. Solids* 39 (1991) 745–762.
- [19] A.I. Lur'e, *Three Dimensional Problems of the Theory of Elasticity*, Interscience Publ., New York, 1964.
- [20] J.A. Wang, J. Lubliner, P.J.M. Monteiro, Effect of ice formation on the elastic moduli of cement paste and mortar, *Cem. Concr. Res.* 18 (6) (1988) 874–885.
- [21] C.M. Neubauer, H.M. Jennings, E.J. Garboczi, A three-phase model of the elastic and shrinkage properties of mortar, *Adv. Cem. Based Mater.* 4 (1996) 6–20.